



Article

Comparison between Measured and Calculated Thermal Conductivities within Different Grain Size Classes and Their Related Depth Ranges

David Bertermann * , Johannes Müller , Simon Freitag and Hans Schwarz

GeoCentre of Northern Bavaria, Friedrich-Alexander-University Erlangen-Nuremberg, Schlossgarten 5, 91054 Erlangen, Germany; johannes.j.mueller@fau.de (J.M.); simon.s.freitag@fau.de (S.F.); hans.schwarz@fau.de (H.S.)

* Correspondence: david.bertermann@fau.de; Tel.: +49-9131-85-25824

Received: 14 June 2018; Accepted: 25 August 2018; Published: 1 September 2018



Abstract: In the field of the efficiency of very shallow geothermal energy systems, there is still a significant need for research activity. To ensure the proper exploitation of this energy resource, the decisive geophysical parameters of soil must be well-known. Within this study, thermal conductivity, as a fundamental property for evaluating the geothermal potential of very shallow geothermal systems, was analyzed and measured with a TK04 device. A dataset, consisting of various geophysical parameters (thermal conductivity, bulk density, water content, and porosity) determined for a large range of different textural soil classes, was collated. In a new approach, the geophysical properties were visualized covering the complete grain size range. The comparison between the measured and calculated thermal conductivity values enabled an investigation with respect to the validity of the different Kersten equations. In the course of this comparison, the influence of effective bulk density was taken into account. In conclusion, both Kersten formulas should be used as recommended and regular bulk density corresponded better to the reference dataset representing the outcomes of the TK04 laboratory measurement. Another objective was to visualize the relation of thermal conductivities within their corresponding textural classes and the validity of Kersten formulas for various bulk densities, depths, and soils. As a result, the accessibility to information for expedient recommendations about the feasibility of very shallow geothermal systems will be improved. Easy, accessible know-how of the fundamentals is important for a growing renewable energy sector where very shallow geothermal installations can also cover heating and cooling demands.

Keywords: soil properties; thermal conductivity; bulk density; textural soil classes; TK04 measurements

1. Introduction

Due to climate change and the consequent societal rethinking about energy policies in favor of renewable energies, geothermal energy has become progressively important for heating and cooling demands. One critical issue of facing global warming by using geothermal applications is the reduction of emitted greenhouse gases [1–3]. To enable proper and sustainable implementation in today's energy concepts, research into geothermal systems is fundamental. Compared to solar or wind energy, geothermal systems—as part of the renewable energy sector—are not dependent on diurnal varying climatic conditions. These systems are only affected by seasonal temperature changes until a certain depth [4]. Thus, these systems are available at any time and are sustainable if anticipatorily used [5]. Furthermore, low enthalpy geothermal systems can be installed almost everywhere to enable a decentralized energy supply. In vertical shallow geothermal systems (up to 400 m in depth),

the thermal conductivity of unconsolidated soil materials only affects the topmost layers. As the contact area between the vertical geothermal systems and the surrounding unconsolidated soil is very small in relation to the total contact area of the whole installed system, the soil's geothermal potential within the vertical installations is much less decisive. For these geothermal installations, the thermal properties of the underlying bedrock are essential.

In the field of unconsolidated soil, primarily horizontal geothermal systems like collector systems or special forms such as heat baskets come into play to exploit this very shallow geothermal potential (vSGP). The vSGP is defined as the natural thermal potential of unconsolidated soil from the surface down to the bedrock [6]. Within the very shallow geothermal sector, the output of such geothermal systems hinges substantially on the thermal conductivity of the surrounding soil. Knowledge on the thermal conductivity of soil materials is one key to elaborate the feasibility and dimension of very shallow geothermal systems [7–9]. The installation of those horizontal systems does not necessarily require drilling operations and consequently, there is most likely to be no interaction of the system with a water aquifer. As a result, only a limited amount of legislation has to be considered. Hence, the dependency on public authorities, or rather, on environmental legislation for shallow geothermal use [10] and the incurred costs are diminished.

The thermal conductivity of soil is also essential for other soil applications. For example, in the field of buried electrical cables, thermal conductivity is a major parameter [11–14]. Particularly, along with the expansion of national and cross-border power grids with high voltage power cables [15,16], this soil parameter is a subject of remarkable interest as the installation depth of high voltage power lines is equivalent to very shallow; i.e., in horizontal geothermal applications. In this case, the thermal properties of the backfilling material also has to be of concern [17,18].

The thermal conductivity of unconsolidated soils depends specifically on soil texture and its pore filling material as well as its mineralogy [19–21]. Taking the mineralogy solely into account, quartz has a significantly better thermal conductivity than clay minerals [22–24]. The soil structure is influenced by various factors like the content of organic matter or the amount of clay [25,26]. In this context, the most relevant parameters are bulk density, soil moisture content, and grain size distribution [27–30], since neither organic content nor carbonates were present within the investigated soil samples.

Within this study, the main topic was the investigation and visualization of the thermal conductivity of soil with respect to other essential geophysical parameters. Reference values, compiled as part of the former ThermoMap project [7] were used. To determine thermal conductivity (λ), common formulas according to Kersten (1949) were used similarly to the ThermoMap project. These equations are based on these three relevant input parameters: bulk density (ρ_b), total volumetric water content (θ_w), and grain size distribution (Equations (1) and (2)). The granulometry, as third relevant parameter, is reflected within the differentiation of both formulas. Equation (1) has to be applied if soils contain more than 50% sand and Equation (2) if soils consist of more than 50% of silt and clay [24,30]. It has to be considered that the following formulas are only valid for unfrozen soil conditions. Although there are other approaches for determining thermal conductivity [19,31–35], to be able to compare the outcomes with other studies, the approach of Kersten (1949) was applied. Additionally, when compared to many other models, the approach used enables its application on all textural soil classes.

$$\lambda = 0.1442 \times (0.7 \times \log(\theta_w / \rho_b) + 0.4) \times 10^{0.6243 \times \rho_b} \quad (1)$$

$$\lambda = 0.1442 \times (0.9 \times \log(\theta_w / \rho_b) - 0.2) \times 10^{0.6243 \times \rho_b} \quad (2)$$

The thermal conductivity of soil can usually be measured with a needle probe at one finite point. Such measurements only cover a few centimeters of the soil around the probes and most of the probes are roughly 10 cm long [36]. To obtain an overview about a large-scale soil body, many measurements are needed. Furthermore, measurements within a depth of more than 15 cm are difficult to perform without soil removal or heavy machinery [37]. With these methods, extensive and

costly (excavation) work has to be executed to obtain representative results in order to analyze the undisturbed thermal conductivity over a depth of several meters. In terms of customized solutions and adapted dimensioning of large-scale, very shallow geothermal systems; however, soil assessment of high accuracy is essential.

In this regard, the analysis of the thermal conductivity of soils within this study should enable an improved soil assessment; i.e., by providing easily accessible visualized correlations between thermal conductivity and soil textural classes. Thermal conductivity has been mainly examined with respect to bulk density, water content, and grain size distribution. A possible application for the usage of effective bulk density with a special focus on clay content was also reflected. To classify the measured results, they were compared with the calculated values of the ThermoMap project [7]. Using these correlations, more convenient thermal conductivity soil investigations can be applied worldwide on any type of soil that is covered by the United States Department of Agriculture (USDA) soil texture classification system [38].

It has to be considered that in this study, due to the TK04 measurements, a stationary system under saturated conditions was investigated. Such circumstances are commonly used to describe the thermal conductivity of soil [19,24,34,35]. However, within a dynamic system like very shallow geothermal installations or buried power lines where significant differences in temperature occur, thermal conductivity is also water flow (vapor diffusion, capillary transport, and convection) dependent [39]. This produces different water flow patterns within soil [40] and consolidated material [41].

2. Materials and Methods

In this study, 61 samples corresponding to nine different soil classes according to the USDA soil texture classification were analyzed. The origin of the samples were the two major German test sites of the ThermoMap project. Both areas, Röttenbach and Büchenbach, are located in the vicinity of Erlangen. Each site is characterized by quaternary, fluvial, and sedimentary deposits. Each sample was tested for its bulk density, water content, and thermal conductivity as well as grain size distribution. By determining the grain size distribution, all investigated samples could be classified using the USDA soil classification. With the mentioned parameters, porosity could be derived. In addition, the feasibility of effective bulk density for thermal conductivity calculations was checked. Subsequently, these data were compared with the calculated thermal conductivity values according to Kersten (1949) and the final lookup table developed within the ThermoMap project [7].

2.1. Soil Parameter

Bulk density ρ_b , is represented by the ratio of mass of soil substances to occupied volume as given by Equation (3).

$$\rho_b = m_d / V_c \quad (3)$$

where m_d gives the dry mass and V_c is the volume of the TK04 cylinder containing the soil sample. The bulk density of the investigated samples was determined as described in the next section following DIN 18125-2 and classified according to Table 1.

Table 1. Classification of bulk density ranges according to [42].

Classification	Bulk Density [g/cm ³]
very low	<1.2
low	1.2–1.4
medium	1.4–1.6
high	1.6–1.8
very high	>1.8

In this study, the effective bulk density, $\rho_{b, \text{eff}}$, was also determined and compared with the regular bulk density. The difference between the effective and normal bulk density depends on the amount of clay content n_c (Equation (4)) [42].

$$\rho_{b, \text{eff}} = \rho_b + 0.009 \times n_c \quad (4)$$

For each soil sample, its grain size distribution was determined. First, the sand fraction was separated by wet sieving according to DIN ISO 11277. After the sieving process, the remaining soil fractions of clay and silt were measured using the Sedigraph III V1.04 (Micromeritics Instrument Corporation, Norcross, GA, USA) to determine the percentage proportions of grain fractions from clay up to fine sand. The Sedigraph utilizes Stoke's law of sedimentation and Beer's law of extinction to separate the different soil fractions. The instrument operates with X-rays to detect the gravity influenced sedimentation process. For these measurements, the samples' particle density was 2.60 g cm^{-3} and the analysis temperature $35 \text{ }^\circ\text{C}$. Porosity (ϕ) can be calculated from the bulk density and density of the soil components (ρ_s) (Equation (5)):

$$\phi = (1 - \rho_b / \rho_s) \quad (5)$$

As the majority of the sandy substrate consists of quartz grains, for ρ_s , the same density as quartz (2.65 g cm^{-3}) was assumed. To consider the computed porosity, the amount of saturated pore volume (S_p) can be determined using the following equation (Equation (6)) [43].

$$S_p = \theta_w / \phi \quad (6)$$

2.2. Thermal Conductivity Measurements

The thermal conductivity of all soil samples was measured with the TK04 half-space probe from TeKa Thermophysical Instrument—Geothermal Investigation using the methodology in ASTM D5334-08. The numeric principles of the used device are based on a line source theory developed by Blackwell in 1954 [44]. First, the samples had to be dried in a drying chamber at $105 \text{ }^\circ\text{C}$ for 24 h to ensure complete dehydration. After determining the dry weight, distilled water was added to the sample until all grains were floating in the water body when mixed. The saturated soil sample was then filled into an iron half space cylinder with known internal dimensions and predetermined weight. The cap, containing the temperature sensor and the heating unit, was inserted upon this cylinder filled with soil material and its total weight was measured. A vertical pressure of 1 MPa was applied, pushing the cap onto the soil sample. The difference in height between the cap's surface and the top of the cylinder was ascertained. These dimensions and the actual weights were used to compute the bulk density. It is important that there are no cavities below the cap, which would lead to incorrect results. In the case of correct preparations, the settings of the measurement program have to be adjusted. For each sample, ten repetitions with cooling intervals of 10 min in between were performed to ensure reproducible results. The TK04 can analyze up to 99 successive repeat measurements for a certain sample adjustment in order to make precision improvements [45].

2.3. Data Analysis

For each soil, classified by the USDA soil texture classification, the analyzed soil properties (bulk density and water content) were correlated to the respective thermal conductivity. Taking these parameters into consideration, thermal conductivity was calculated by using Equations (1) and (2) after Kersten (1949) and Farouki (1981) [24,30]. These calculations were also performed with the effective bulk density. To check the validity of both Kersten formulas (Equations (1) and (2)), the thermal conductivity of all samples was calculated with both equations, regardless of their granulometry. These differently calculated and measured thermal conductivities were then compared. Additionally, other standardized thermal conductivity values of the European ThermoMap project [8] were added to the analysis to classify the thermal conductivities under distinct saturated conditions. In the

ThermoMap project, the thermal conductivity values were also calculated using the formulas after Kersten (1949) [7]. In the course of this project, thermal conductivity was associated to three different bulk densities: 1.3 g cm^{-3} , 1.5 g cm^{-3} , and 1.8 g cm^{-3} . By comparing the values according to the ThermoMap project with the measured thermal conductivities, the best fit between the calculated and measured thermal conductivity values can be assessed.

Furthermore, the TK04 measurements were compared to the expected thermal conductivities calculated according to Kersten (1949) and Farouki (1981), distinguishing between sand- (Equation (1)) and silt-/clay-dominated (Equation (2)) soils. Additionally, the effect of applying the effective bulk density (Equation (4)) on the Kersten equation was determined.

2.4. Data Projection

To visualize the data in an interrelated way with a focus on the USDA soil texture classification, it was integrated into a GIS software. The spatial position of each data point within the USDA textural classification diagram, an equilateral ternary plot, was defined by a triple of data (i.e., % sand/% silt/% clay). To transfer these spatial data into a GIS software, the data triples were transferred into Cartesian coordinates (i.e., 100% sand = (0,0); 100% silt = (0,1); 100% clay = $(1/2, \sqrt{3}/2)$).

All 61 samples were imported to ArcMap using the X-/Y-values as described above. Two reference points were added to the dataset to visualize 100% sand (0,0) and 100% silt (0,1), and to create a common working base for further interpolations (Figure 1).

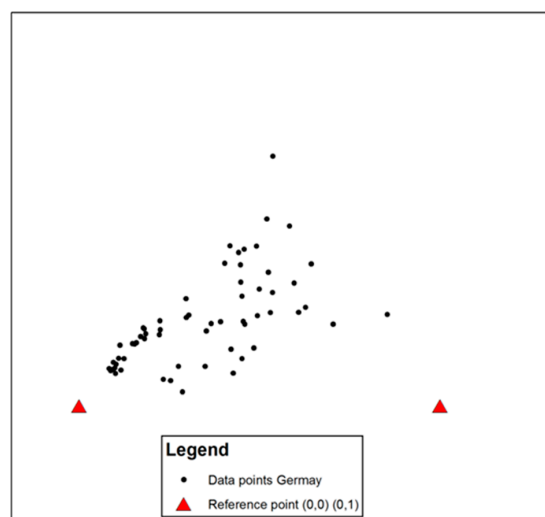


Figure 1. Visualization of the shapefile used for further interpolations.

To obtain a coherent distribution within the ternary plot, the data was interpolated. To be able to later apply statistical algorithms, the inverse distance weighting (IDW) algorithm was selected to receive an interpolated raster surface. The IDW was used since the data were located relatively close to each other and, furthermore, the IDW is limited to the range of raw data [46]. The searching radius was set to variable and the number of points within the search radius settings was set to 30 for each ternary plot.

Using this procedure, the three measured soil parameters, bulk density, porosity, and thermal conductivity as well as the comparisons between the measured and calculated thermal conductivities, were plotted. Furthermore, various plots with deviations between different thermal conductivities were generated: first, a comparison between the measured thermal conductivities and values calculated after Kersten (1949); second, a comparison between the measured thermal conductivity TK04 results and the values of the lookup table of the ThermoMap project including the three bulk density stages (see Section 3). The classification for the bulk density plot is based on Sponagel (2005) (Table 1).

3. Results

A summary of the measured results is displayed in Table 2. Based on the grain size distribution, nine different grain size classes according to the USDA soil texture classification from various locations (inside Germany) were examined in terms of bulk density, porosity, and thermal conductivity.

Table 2. Data table with the results of all samples investigated. Bulk density and one thermal conductivity (TK04-column) were measured by the TK04 device. Porosity and thermal conductivity according to Kersten (1949) were both computed based on the outcomes of the performed measurements of this study. The third calculated thermal conductivity was provided by the ThermoMap project. Textural soil classes were derived based on the samples granulometry.

Sample-ID	Textural Soil Class	Bulk Density [g/cm ³]	Porosity [%]	Thermal Conductivity [W (m·K) ⁻¹]	
				TK04	Kersten (1949)
I3	Loamy Sand	1.060	60.0	2.197	1.088
II2b	Sandy Loam	1.561	41.0	1.834	2.080
II3a	Loamy Sand	1.723	35.0	2.318	2.542
III2a	Sandy Clay Loam	1.598	40.0	1.771	2.179
III2b	Sandy Clay Loam	1.836	31.0	2.426	2.910
III3a	Sandy Clay Loam	1.503	43.0	1.398	1.934
III3b	Clay Loam	1.246	53.0	1.429	1.169
III4b	Sandy Clay Loam	1.672	37.0	1.912	2.388
III5a	Clay	1.359	49.0	0.959	1.341
III5b	Sandy Loam	1.707	36.0	2.019	2.493
IV2b	Clay	0.959	64.0	0.906	0.815
IV3a	Clay	1.185	55.0	1.147	1.084
IV3b	Clay	1.134	57.0	1.188	1.017
IV4	Clay	1.134	57.0	1.152	1.017
RD2	Clay	1.085	54.6	1.241	0.936
RD3	Clay	1.106	52.6	1.183	0.954
RD4	Clay	1.078	50.4	1.266	0.904
RD5	Sandy Loam	1.547	24.6	1.704	1.831
RD6	Clay Loam	1.071	56.2	1.169	0.924
RD7	Loam	1.209	45.2	1.293	1.057
RE1	Sandy Clay Loam	1.595	23.9	2.020	1.949
RE2	Sandy Clay Loam	1.532	26.6	2.065	1.823
RE3	Sandy Clay Loam	1.718	21.0	2.285	2.258
RE4	Sandy Loam	1.644	22.9	2.173	2.072
RE5	Sandy Clay Loam	1.624	23.6	1.873	2.025
RE6	Sandy Loam	1.629	23.6	2.070	2.041
RF1	Sandy Clay Loam	1.483	28.9	1.875	1.730
RF2	Loamy Sand	1.694	20.5	2.412	2.170
RF3	Loamy Sand	1.560	25.5	1.687	1.880
RF4	Sandy Loam	1.694	21.0	2.413	2.182
RF5	Loamy Sand	1.545	26.5	2.189	1.856
RF6	Loamy Sand	1.538	26.9	2.037	1.844
RF7	Loamy Sand	1.544	26.1	2.192	1.845
RI-2	Silt Loam	1.260	52.4	1.157	1.189
RI-5	Sandy Clay Loam	1.590	39.9	1.666	2.156
RIII-2	Silty Clay	1.450	45.1	1.138	1.494
RIII-5	Clay Loam	1.360	43.0	1.317	1.294
RIV-1b	Sandy Clay Loam	1.280	51.6	1.355	1.452
RIV-2	Clay Loam	1.210	54.5	1.180	1.119
RIV-4	Clay Loam	1.440	45.6	1.281	1.478
RIX-1	Clay	1.100	58.4	1.098	0.974
RVIII-2	Loamy Sand	1.770	33.1	2.435	2.688
V2	Sandy Loam	1.667	37.0	1.921	2.373
VA2	Clay Loam	1.340	43.0	1.407	1.257
VA3	Clay Loam	1.560	43.0	1.762	1.725
VA4	Clay Loam	1.430	43.0	1.345	1.431

Table 2. Cont.

Sample-ID	Textural Soil Class	Bulk Density [g/cm ³]	Porosity [%]	Thermal Conductivity [W (m·K) ⁻¹]	
				TK04	Kersten (1949)
VA5	Loam	1.490	42.0	1.487	1.548
VA6	Sandy Loam	1.650	52.0	1.616	2.475
VA7	Sandy Loam	1.650	43.0	1.665	2.385
VA8	Sandy Loam	1.660	52.0	1.674	2.510
VA9	Sandy Loam	1.620	36.0	1.581	2.205
VB1	Sandy Clay Loam	1.470	35.0	1.230	1.767
VB10	Sandy Loam	1.590	54.0	1.591	2.286
VB2	Clay Loam	1.210	43.0	1.477	1.043
VB3	Sandy Clay Loam	1.360	54.0	1.517	1.384
VB5	Loam	1.300	36.0	1.408	1.122
VB6	Loam	1.270	42.0	1.352	1.129
VB7	Silty Clay Loam	1.360	48.8	1.257	1.344
VB8	Loam	1.430	43.0	1.466	1.431
VB9	Loam	1.410	54.0	1.426	1.488
VI3b	Sandy Loam	1.723	35.0	2.378	2.542

3.1. Bulk Density and Porosity

In general, clayey soils are classified as having low and very low bulk densities (Table 1), ranging from 0.959 g cm⁻³ up to 1.359 g cm⁻³ (Table 2) with an average of 1.127 g cm⁻³. Elevated bulk density values could be observed with an increasing proportion of sand (Figure 2). For sandy clay loam samples, high and marginally very high bulk densities were measured, reaching values of 1.836 g cm⁻³. However, the range of bulk density within each grain size class was quite large, as observable within the loamy sands or clays.

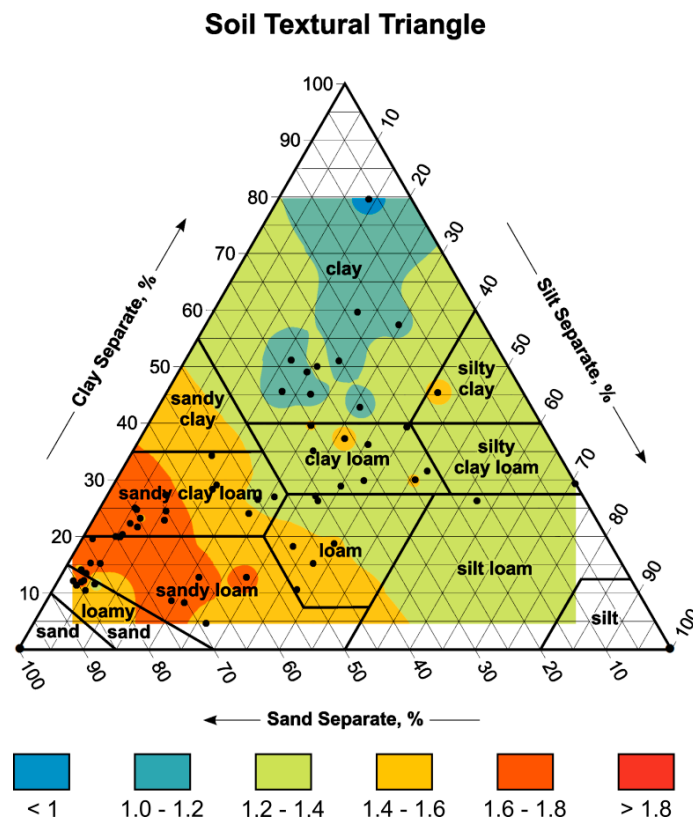


Figure 2. Bulk density [g cm⁻³] distribution dependent on the textural soil classification.

The computed porosities showed an inverse trend when compared to the bulk density (Figure 3), which was not remarkable/surprising since the calculation was based on the measured bulk densities. Porosity decreased with an increasing content of sand. A minimum porosity of 20.5% appeared for loamy sands- and sandy clay loams. Clays, in particular, showed the highest porosities.

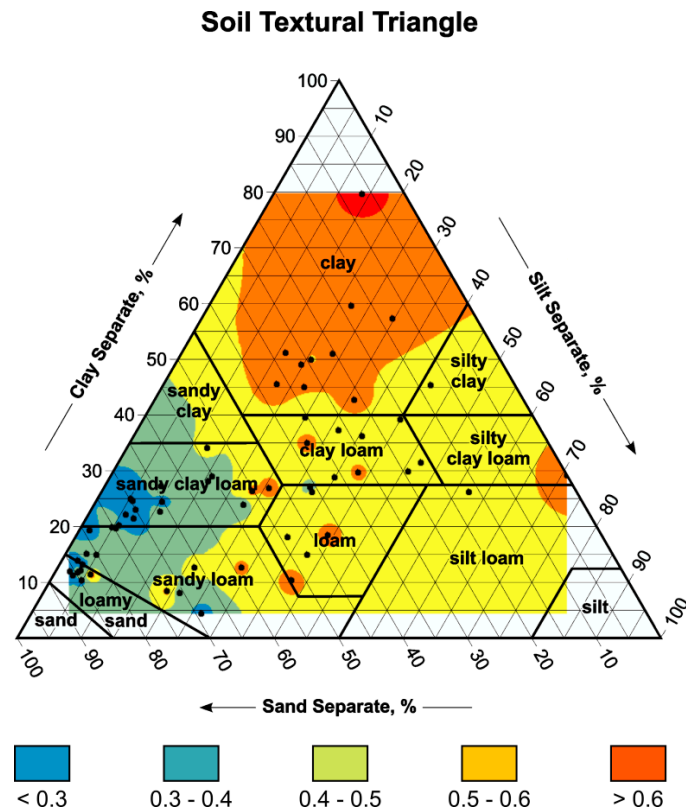


Figure 3. Distribution of porosity [-] dependent on the USDA textural soil classification.

3.2. Thermal Conductivity

The two major objectives in this study focused, on the one hand, on the comparison between the measured thermal conductivity values with the TK04 device and the calculated thermal conductivity values when different Kersten formulas were applied (Section 3.2.2). On the other hand, a comparison of the thermal conductivity values with the TK04-measured device and the calculated ThermoMap values for the three different bulk density values (Section 3.2.3) was performed.

3.2.1. Thermal Conductivity Measurements

Figure 4 displays the distribution of thermal conductivity within the USDA soil texture classification. In this case, the coarse material showed higher thermal conductivity values than the fine material.

Regardless of the grain size classes, all measured thermal conductivities were in a range between $0.906 \text{ W (m}\cdot\text{K)}^{-1}$ and $2.435 \text{ W (m}\cdot\text{K)}^{-1}$ (Table 2). In this range, clay possessed the lowest values, whereas loamy sand and sandy loam showed very high thermal conductivities. However, the spread of the thermal conductivity in the 'loamy sand' and 'sandy loam' section was relatively high, as they covered a range from $1.581 \text{ W (m}\cdot\text{K)}^{-1}$ up to $2.435 \text{ W (m}\cdot\text{K)}^{-1}$. This was accompanied by a positive correlation with increasing bulk density (Figure 5).

A positive correlation of thermal conductivity with increasing sand content was observed (Figure 4) as well as a positive correlation between the bulk densities and increasing sand content (Figure 2). Hence, the relation between thermal conductivity and bulk density as displayed in Figure 5 was not surprising.

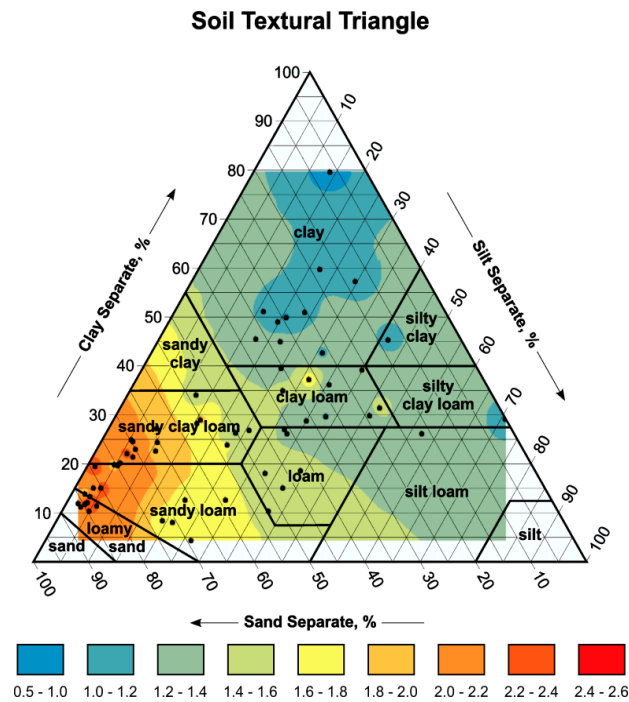


Figure 4. Distribution of measured thermal conductivity $[W (m \cdot K)^{-1}]$ for the different textural soil classes.

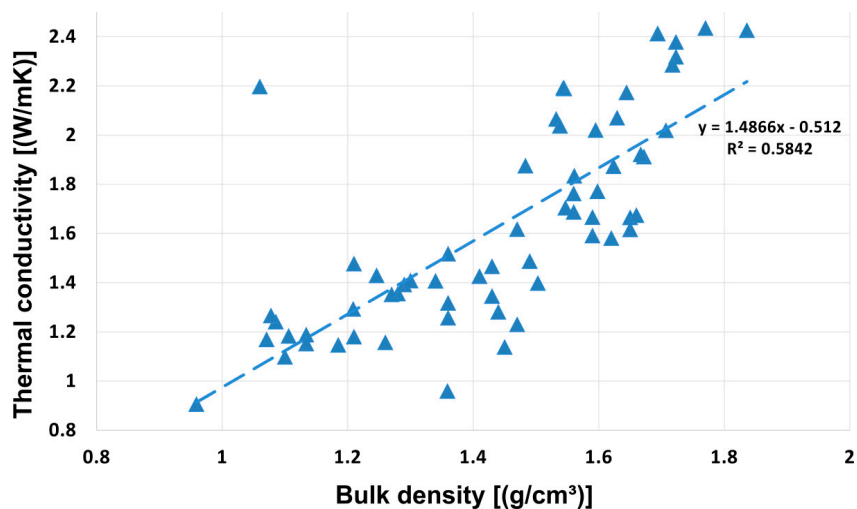
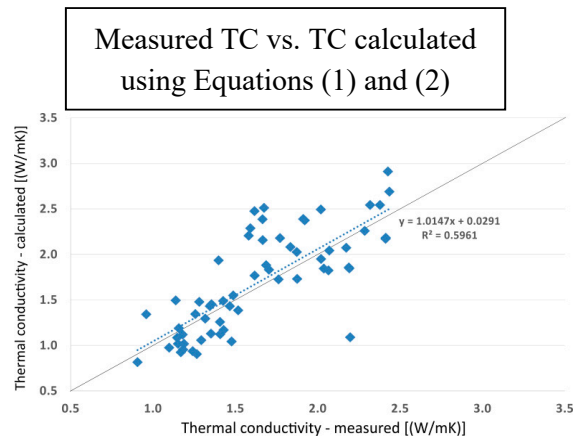
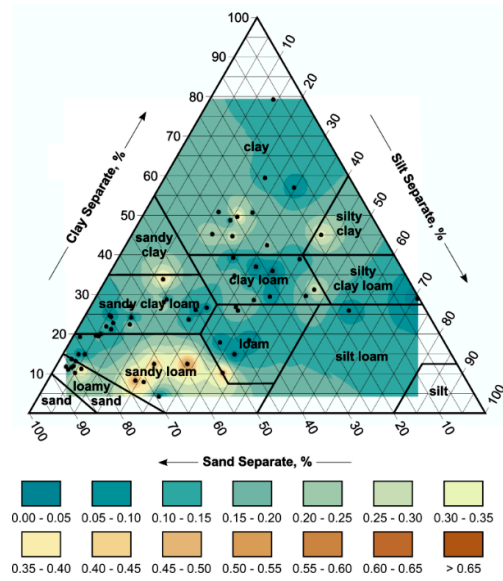


Figure 5. Bulk density plotted against the thermal conductivities measured with the TK04.

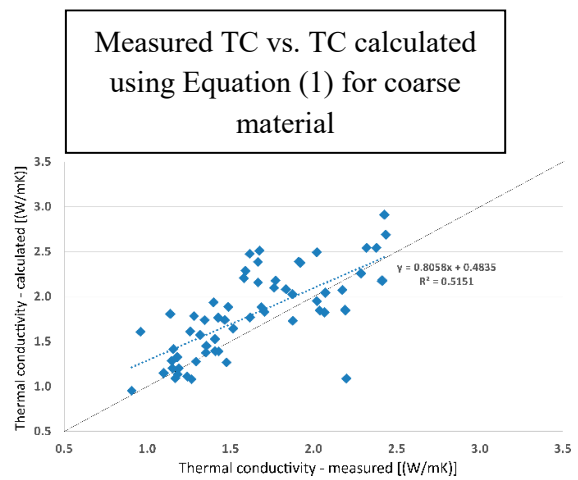
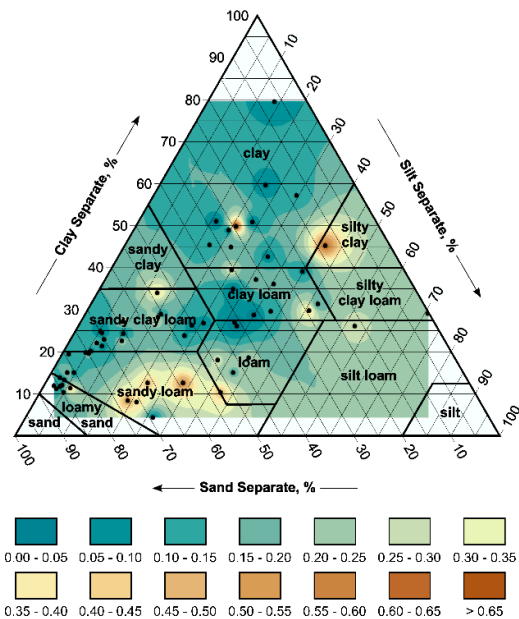
3.2.2. Thermal Conductivity Measurements vs. Kersten Formulas

The best correlation between the measured and calculated thermal conductivity could be achieved by applying the formulas from Kersten (1949), distinguishing between sand- (Equation (1)) and silt-/clay-dominated (Equation (2)) soils as recommended, and using the measured bulk densities for calculation (Figure 6b). When applying only Equation (1) for the sand-dominated soils, the associated regression line showed a pronounced discrepancy from the line through the origin (Figure 6d) at lower thermal conductivities. For high thermal conductivities, the regression line converged to the line through the origin. An inverse trend can be observed in Figure 6f, where the thermal conductivity was calculated by only applying Equation (2). In this case, a better correlation between the measured and calculated thermal conductivities was noticed for soils with low thermal conductivities, and with increasing thermal conductivity, the discrepancy increased.

However, these observations could not be confirmed in Figure 6a,c,e where the mentioned deviations within the thermal conductivities were not visible in relation to the USDA soil texture classification. An overall higher deviation between the measured and calculated thermal conductivities is illustrated by the comparison of Figure 6a,c,e. Deviations between the measured and calculated thermal conductivities, by the recommended application of the Kersten formulas (Figure 6a), showed significant differences, especially for sandy loam (up to 0.55–0.60 W (m·K)⁻¹) but also for sandy clay (≤ 0.4 W (m·K)⁻¹), and minor differences for sandy clay and loamy sand (≤ 0.35 W (m·K)⁻¹). Higher contrasts in thermal conductivities, calculated by applying only Equation (1) (Figure 6c), appeared in the areas of sandy loam and silty clay (up to 0.6 W (m·K)⁻¹). The measured thermal conductivities of clay loam, clay as well as sandy clay loam, on the contrary, hardly deviated from the calculated ones. The overall lowest deviations between the calculated and measured thermal conductivities (Figure 6e) occurred by only applying Equation (2). In this case, differences of ≤ 0.35 W (m·K)⁻¹ appeared within the loamy sand and silty clay.

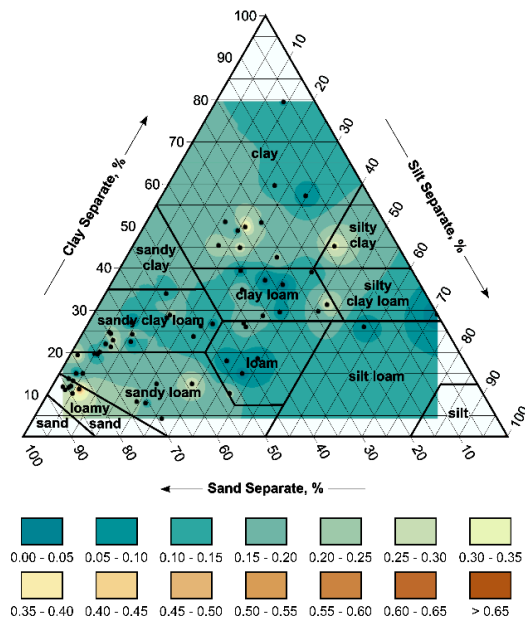


(b)

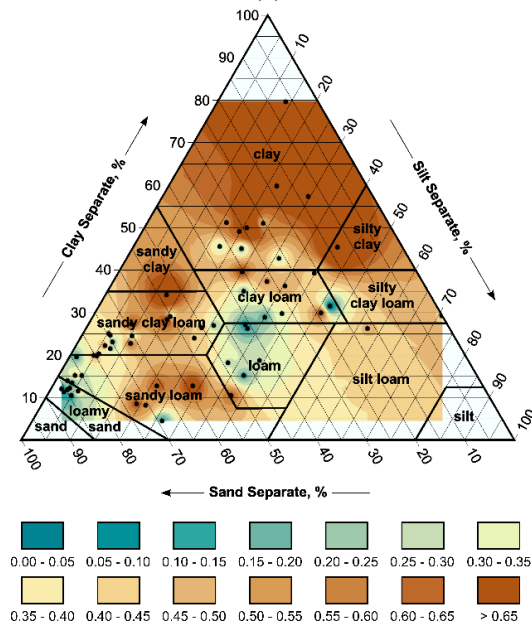


(d)

Figure 6. Cont.

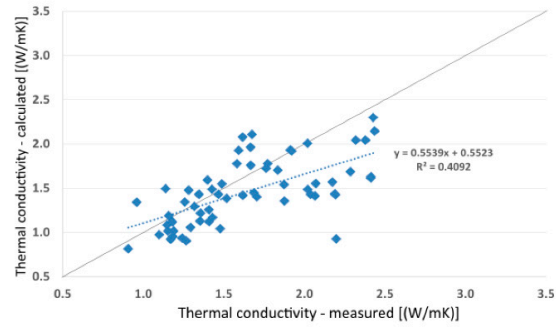


(e)



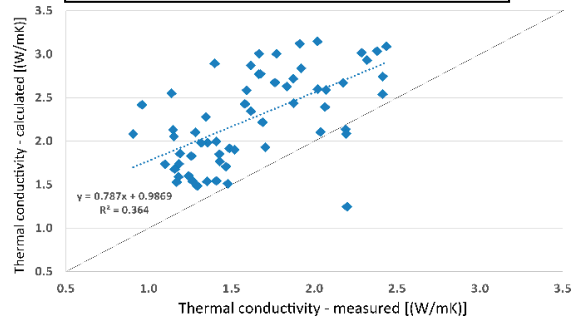
(g)

Measured TC vs. TC calculated using Equation (2) for fine material



(f)

Measured TC vs. TC calculated using both Equations (1) and (2) in consideration of effective bulk density



(h)

Figure 6. (a) Deviation (%) of the thermal conductivity values using the Kersten formulas (Equations (1) and (2)) from the TK04 measurements; (b) Plot of the measured versus the calculated thermal conductivities after Kersten (Equations (1) and (2)) (Linear regression line = black dashed line); (c) Deviation (%) of the thermal conductivity values using the Kersten formula (Equation (1)) from the TK04 measurement; (d) Plot of the measured versus the calculated thermal conductivities after Kersten (Equation (1)) (Linear regression line = black dashed line); (e) Deviation (%) of the thermal conductivity values using the Kersten formula (Equation (2)) from the TK04 measurements; (f) Plot of the measured versus the calculated thermal conductivities after Kersten (Equation (2)) (Linear regression line = black dashed line); (g) Deviation (%) of the thermal conductivity values using the Kersten formulas (Equations (1) and (2)) and effective bulk density values from the TK04 measurements; (h) Plot of the measured versus the calculated thermal conductivities after Kersten using the effective bulk densities instead of standard bulk densities. (Linear regression line = black dashed line).

By calculating the thermal conductivity with the equations according to Kersten (1949) and by using the calculated effective bulk density (Equation (4)) instead of the measured one, a distinct larger gap in relation to the measured thermal conductivity was observable (Figure 6h). The calculated thermal conductivities were accounted/lifted roughly $1.0 \text{ W (m}\cdot\text{K)}^{-1}$ above the measured thermal conductivities. This relationship is also reflected in Figure 6g where a strong deviation between the measured and calculated thermal conductivities was implied. This observation was true for nearly all of the data points and classes, except for some areas within clay loam, loam, and loamy sand.

The calculated thermal conductivities for soils in the uppermost depths stage of 0–3 m and a standardized bulk density of 1.3 g cm^{-3} ranged from $\sim 1.2 \text{ W (m}\cdot\text{K)}^{-1}$ to $\sim 1.5 \text{ W (m}\cdot\text{K)}^{-1}$ (Figure 7). The regression line (Figure 7) had a much lower slope of 0.2107 than the line through the origin.

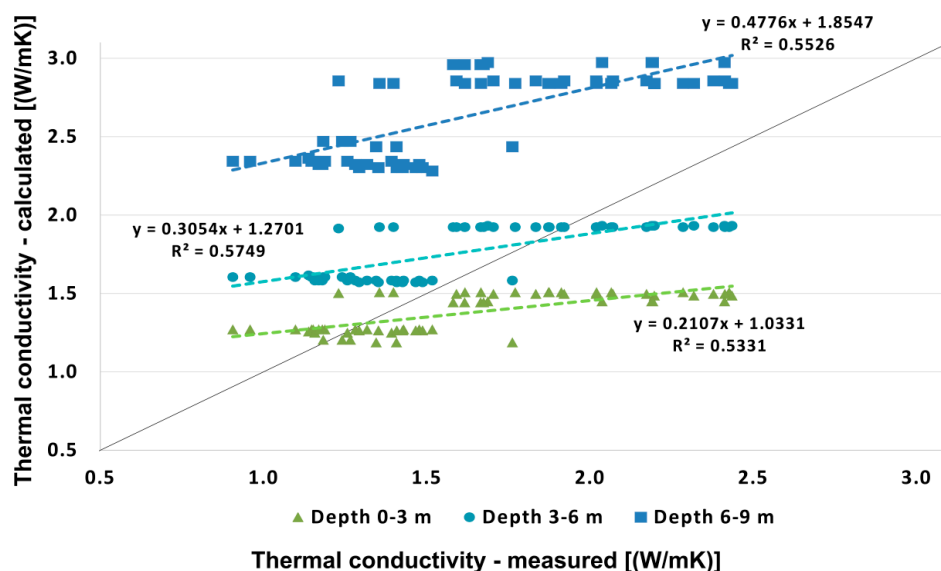


Figure 7. The measured vs. calculated thermal conductivities according to Kersten (1949) for varying soil depths; i.e., bulk densities according to the ThermoMap project.

3.2.3. Thermal Conductivity Measurements vs. ThermoMap Values

This slight underestimation is also reflected in Figure 8, where positive and negative deviation of the ThermoMap project values from the thermal conductivities measured with the TK04 were related to the USDA soil texture classification. In particular, sand rich areas (loamy sand, sandy loam, and sandy clay loam) strongly deviated negatively (down to $0.42 \text{ W (m}\cdot\text{K)}^{-1}$) from the measured values. In contrast, clays were rather overestimated with a difference in thermal conductivity of up to $0.30 \text{ W (m}\cdot\text{K)}^{-1}$. By using a standardized bulk density of 1.5 g cm^{-3} , representing soils at depths of 3–6 m, for calculating thermal conductivity after Kersten (1949), a better fit was achieved. The values generally deviated less from the best fit when compared to the ones calculated for a depth range of 0–3 m. However, a general overestimation of the calculated thermal conductivities calculated with a standardized bulk density of 1.5 g cm^{-3} was observed in Figure 9. A maximum positive deviation of $0.55 \text{ W (m}\cdot\text{K)}^{-1}$ was reached for clay, whereas loamy sand, sandy loam, and sandy clay loam were still underestimated (down to $-0.27 \text{ W (m}\cdot\text{K)}^{-1}$). The thermal conductivities calculated for soils at a depth of 6–9 m, with an expected bulk density of 1.8 g cm^{-3} , generally showed an unfavorable correlation with the measured thermal conductivity values (Figure 7). This was reflected in the calculated thermal conductivities deviating at least $\sim 0.4 \text{ W (m}\cdot\text{K)}^{-1}$ from the highest and $\sim 1.3 \text{ W (m}\cdot\text{K)}^{-1}$ from the lowest measured thermal conductivities.

The databases for Figures 8–10 are listed in an overview table (Table 3) where the thermal conductivity values for all respective bulk densities, which were defined in the ThermoMap project, were collated.

Table 3. TK04-measured thermal conductivities (TC) for each classified soil sample and three calculated ThermoMap thermal conductivity values; each column has one single bulk density (BD) value. The three different bulk density values represent the depth layers 0–3 m, 3–6 m, and 6–10 m [7].

Sample-ID	Textural Soil Class	TC (TK04) [W/(m·K)]	TC ThermoMap [W (m·K) ⁻¹] (BD = 1.3 g cm ⁻³)	TC ThermoMap [W (m·K) ⁻¹] (BD = 1.5 g cm ⁻³)	TC ThermoMap [W (m·K) ⁻¹] (BD = 1.8 g cm ⁻³)
I3	Loamy Sand	2.197	1.41	1.78	2.50
II2b	Sandy Loam	1.834	1.42	1.77	2.51
II3a	Loamy Sand	2.318	1.41	1.78	2.50
III2a	Sandy Clay Loam	1.771	1.43	1.77	2.50
III2b	Sandy Clay Loam	2.426	1.43	1.77	2.50
III3a	Sandy Clay Loam	1.398	1.43	1.77	2.50
III3b	Clay Loam	1.429	1.17	1.38	1.88
III4b	Sandy Clay Loam	1.912	1.43	1.77	2.50
III5a	Clay	0.959	1.17	1.41	1.90
III5b	Sandy Loam	2.019	1.42	1.77	2.51
IV2b	Clay	0.906	1.17	1.41	1.90
IV3a	Clay	1.147	1.17	1.41	1.90
IV3b	Clay	1.188	1.17	1.41	1.90
IV4	Clay	1.152	1.17	1.41	1.90
RD2	Clay	1.241	1.17	1.41	1.90
RD3	Clay	1.183	1.17	1.41	1.90
RD4	Clay	1.266	1.17	1.41	1.90
RD5	Sandy Loam	1.704	1.42	1.77	2.51
RD6	Clay Loam	1.169	1.17	1.38	1.88
RD7	Loam	1.293	1.17	1.37	1.86
RE1	Sandy Clay Loam	2.020	1.43	1.77	2.50
RE2	Sandy Clay Loam	2.065	1.43	1.77	2.50
RE3	Sandy Clay Loam	2.285	1.43	1.77	2.50
RE4	Sandy Loam	2.173	1.42	1.77	2.51
RE5	Sandy Clay Loam	1.873	1.43	1.77	2.50
RE6	Sandy Loam	2.070	1.42	1.77	2.51
RF1	Sandy Clay Loam	1.875	1.43	1.77	2.50
RF2	Loamy Sand	2.412	1.41	1.78	2.50
RF3	Loamy Sand	1.687	1.41	1.78	2.50
RF4	Sandy Loam	2.413	1.42	1.77	2.51
RF5	Loamy Sand	2.189	1.41	1.78	2.50
RF6	Loamy Sand	2.037	1.41	1.78	2.50
RF7	Loamy Sand	2.192	1.41	1.78	2.50
RI-2	Silt Loam	1.157	1.15	1.38	1.90
RI-5	Sandy Clay Loam	1.666	1.43	1.77	2.50
RIII-2	Silty Clay	1.138	1.16	1.42	1.92
RIII-5	Clay Loam	1.317	1.17	1.38	1.88
RIV-1b	Sandy Clay Loam	1.355	1.43	1.77	2.50
RIV-2	Clay Loam	1.180	1.17	1.38	1.88
RIV-4	Clay Loam	1.281	1.17	1.38	1.88
RIX-1	Clay	1.098	1.17	1.41	1.90
RVIII-2	Loamy Sand	2.435	1.41	1.78	2.50
V2	Sandy Loam	1.921	1.42	1.77	2.51
VA2	Clay Loam	1.407	1.17	1.38	1.88
VA3	Clay Loam	1.762	1.17	1.38	1.88
VA4	Clay Loam	1.345	1.17	1.38	1.88
VA5	Loam	1.487	1.17	1.37	1.86
VA6	Sandy Loam	1.616	1.42	1.77	2.51
VA7	Sandy Loam	1.665	1.42	1.77	2.51
VA8	Sandy Loam	1.674	1.42	1.77	2.51
VA9	Sandy Loam	1.581	1.42	1.77	2.51
VB1	Sandy Clay Loam	1.230	1.43	1.77	2.50
VB10	Sandy Loam	1.591	1.42	1.77	2.51
VB2	Clay Loam	1.477	1.17	1.38	1.88

Table 3. Cont.

Sample-ID	Textural Soil Class	TC (TK04) [W/(m·K)]	TC ThermoMap [W (m·K) ⁻¹] (BD = 1.3 g cm ⁻³)	TC ThermoMap [W (m·K) ⁻¹] (BD = 1.5 g cm ⁻³)	TC ThermoMap [W (m·K) ⁻¹] (BD = 1.8 g cm ⁻³)
VB3	Sandy Clay Loam	1.517	1.43	1.77	2.50
VB5	Loam	1.408	1.17	1.37	1.86
VB6	Loam	1.352	1.17	1.37	1.86
VB7	Silty Clay Loam	1.257	1.17	1.40	1.90
VB8	Loam	1.466	1.17	1.37	1.86
VB9	Loam	1.426	1.17	1.37	1.86
VI3b	Sandy Loam	2.378	1.42	1.77	2.51

This observation was confirmed in the soil textural triangle (Figure 10), accounting for a strong positive deviation of up to $1.10 \text{ W (m·K)}^{-1}$ (for clays) calculated from the measured thermal conductivities. The smallest deviations in thermal conductivities were determined for loamy sands, silt-poor sandy loams, and silt-poor sandy clay loams.

When comparing the measured thermal conductivities with the values calculated and sorted after Kersten (1949) (Figure 11), thereby distinguishing between the conventional method using both Equations (1) and (2), and just using either one of the formulas, several observations were apparent. With the exception of two samples, the equation used for the samples with a sand proportion below 50% was applied to all soils with a calculated low thermal conductivity. Whereas for all soils with a calculated high thermal conductivity, the equation for sand proportions above 50% was used. Furthermore, the thermal conductivities calculated solely with Equation (2) always possessed lower values than when calculated with Equation (1). In the area of the lowest thermal conductivities (Section 1/Figure 11), the measured values correlated with the predicted ones that used the Equation (1), although these samples comprised only clayey/silty soils.

Decent accordance was achieved in the middle section between the measured and thermal conductivities predicted with the conventional method. Section 3 shows the measured thermal conductivities that were in agreement with values predicted with Equation (2), despite the samples being sandy soils.

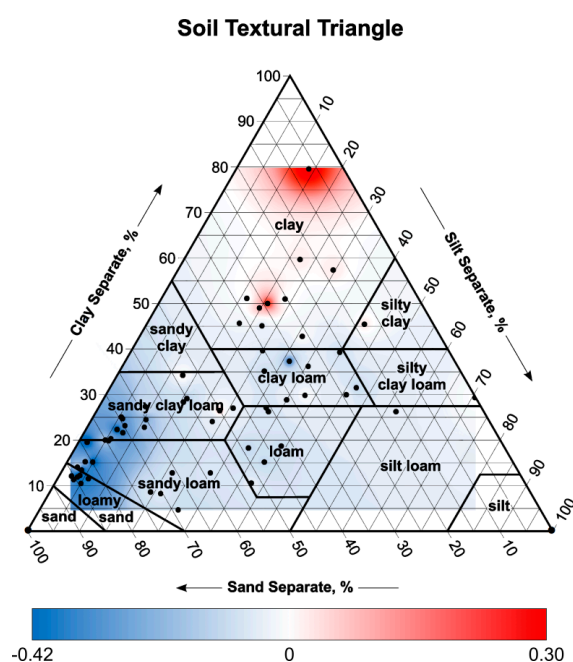


Figure 8. Positive and negative deviation of the ThermoMap values (BD = 1.3 g cm^{-3}) from the TK04 measured thermal conductivities.

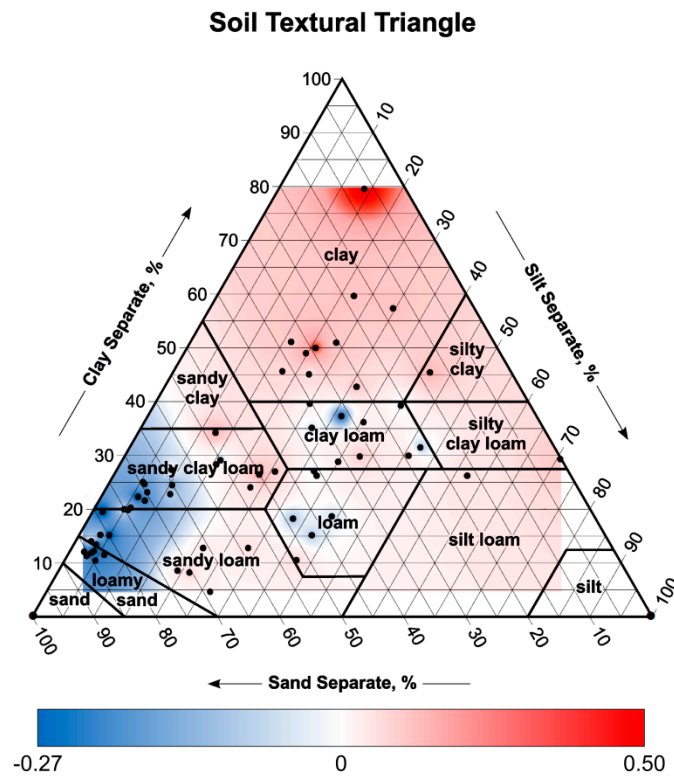


Figure 9. Positive and negative deviation of the ThermoMap values ($BD = 1.5 \text{ g cm}^{-3}$) from the TK04 measured thermal conductivities.

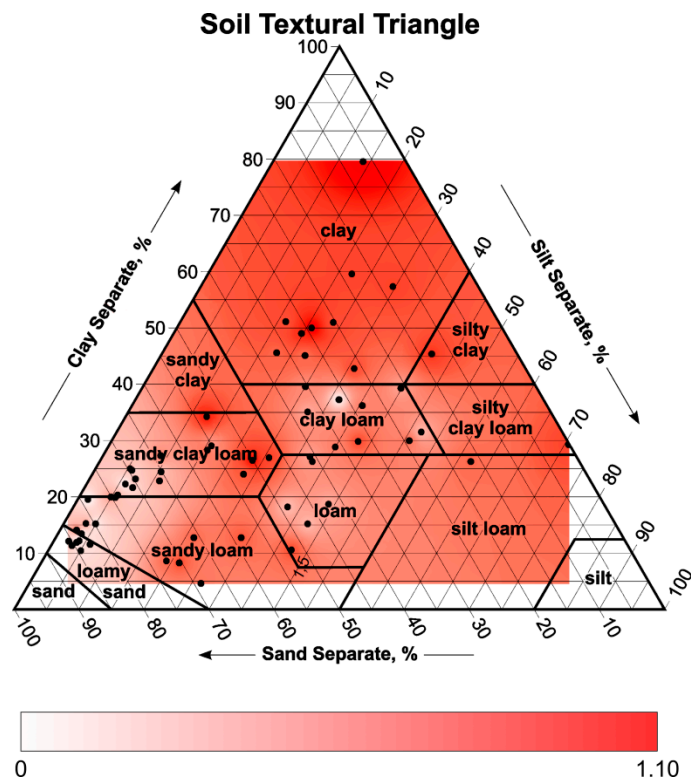


Figure 10. Positive deviation of the ThermoMap values ($BD = 1.8 \text{ g cm}^{-3}$) from the TK04 measured thermal conductivities.

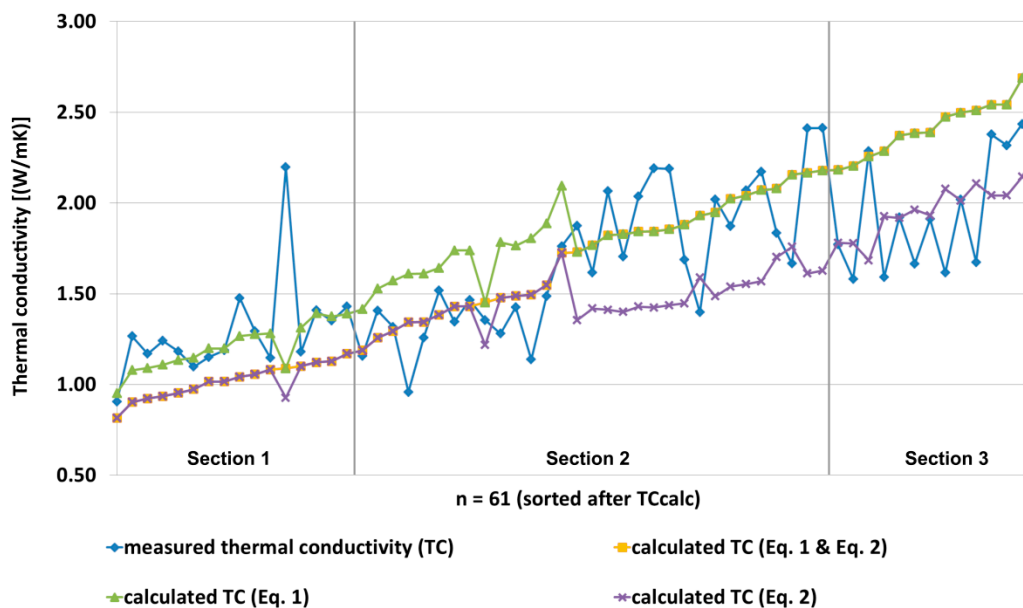


Figure 11. Comparison between the measured (TK04 results) and calculated thermal conductivities. The calculations according to both Kersten (1949) equations are displayed (sand formula, Equation (1); clay formula, Equation (2)). The values were sorted after the calculated thermal conductivity corresponded to both soil dependent formulas (Equation (1) > 50% sand; Equation (2) < 50% sand).

4. Discussion

The aim of this study was to compare the thermal conductivity values derived by the laboratory TK04 measurements and hypothetical soil properties derived from the ThermoMap project and their visualization in USDA textural classes. Bulk densities should preferably be used for thermal conductivity calculations according to Kersten (1949). Generally, for calculating thermal conductivity, a bulk density of about 1.5 g cm^{-3} fits best. However, an even better result was achieved by distinguishing between certain grain size classes and applied bulk densities. Clay soils were represented best by using the bulk density of 1.3 g cm^{-3} (Figure 8), whereas a bulk density of 1.8 g cm^{-3} only provided suitable outcomes for very pure sands (Figure 10). All of the other intermediate grain size classes such as loamy sand, sandy loam, or silts should be calculated with an assumed bulk density of 1.5 g cm^{-3} (Figure 9). These results corresponded to the bulk density ranges stated by Chaudhari et al. (2013), although a high clay content could mask the effect of an increased organic content [1,2]. In contrast to coarse soils [47], clays possess a relatively high porosity, resulting in lower bulk densities.

Computing thermal conductivity with effective bulk density provided unrealistic high values (Figure 6g and Table 2). This was also observed by Renger et al. (2008), who proposed that the calculation factor for computing the effective bulk density of 0.0009 applied in Equation (4) was too high. This may be due to the predominantly medium to high organic content of the soils, where the factor was derived from [48]. Operating with effective bulk densities showed the highest deviations in fine grained soils (Figure 6g), despite having been particularly developed for this fine grain size fraction.

It must be considered that although a consistent pressure load was applied by measuring with the TK04, different bulk densities were generated dependent on the respective compactibility of each grain size class (Figure 3). Still, the relation between bulk density and thermal conductivity showed a low coefficient of correlation (Figure 5). Thus, bulk density does not solely control the thermal conductivity of soils. Other crucial factors are the degree of saturation (θ), volume fraction of air (n) as well as the volume fraction of solids (v_s) [21,28,30,49]. Additionally, mineral type and grain size distribution are decisive for the thermal conductivity of soils [50]. As all samples in this study were measured under saturated conditions, the degree of saturation and volume fraction of air could be neglected.

Moreover, a mineralogical test was not conducted. Consequently, only grain size distribution was taken into account.

Clays and silts, in contrast to sandy soils, have a very high porosity (Figure 4), which results in lower bulk densities [47]. As a consequence, by measuring under saturated conditions, the relative amount of water in clays/silts was much higher than in sandy soils. Water intrinsically has a much lower thermal conductivity of $\sim 0.6 \text{ W (m}\cdot\text{K)}^{-1}$ [51] than most minerals with values $>1.9 \text{ W (m}\cdot\text{K)}^{-1}$. Furthermore, the amount of quartz minerals that possess very high thermal properties of up to $7.7 \text{ W (m}\cdot\text{K)}^{-1}$ [52,53] was lower in clayey/silty than in sandy soils. Altogether, this led to the decreased thermal conductivities of fine grained soils in contrast to sandy soils. The observations made within this study were thereby in agreement with the results of Brigaud and Vasseur (1989) [52]. Referring to the factors investigated in this study such as bulk density, grain size, and mineralogy, Zhang et al. (2017) reported similar results [50]. This regarded the positive correlation between increasing bulk density, particle size, and thermal conductivity.

When the critical moisture content is reached, thermal conductivity does not further increase significantly. According to Zhang et al. (2017), the critical moisture content of clay-/silt-soils is much higher when compared to that of sandy soils. As a consequence, the calculated thermal conductivities representing high water contents or completely saturated soils are likely to be overestimated, especially for sands (Figure 11).

The reason for the larger fluctuations within the sandy soils when compared to the clayey/silty soils was not thoroughly investigated in this study. However, these fluctuations might be caused by mineralogical variations, different bulk densities, or device-related measurement errors. Furthermore, dynamic hydraulic processes were not considered. However, to measure comparable thermal conductivities, a constant water content is crucial.

In times of fossil fuel shortage [54], all research in the fields of renewable energy systems is fundamental to develop alternative energy concepts for heating and cooling, for example, by the usage of geothermal heat pumps that will increase massively over the next few decades [55]. Detailed knowledge about thermo-physical soil properties is notably beneficial when planning very shallow geothermal systems due to their impact on the efficiency of geothermal installations. Research on thermal conductivity, such as this study, is the foundation for a proper soil assessment regarding sustainable energy supply.

5. Conclusions

Under saturated conditions, the higher the amount of sand or quartz grains, respectively, the higher the thermal conductivity of soil. Additionally, a high bulk density significantly improves thermal conductivity. From the comparison of various thermal conductivities with the measured and classified values as well as different calculations using the formulas after Kersten, the following conclusions can be drawn. Regular bulk density provided the best fit with the formulas to calculate thermal conductivity, whereas effective bulk density led to an overestimation. Furthermore, to calculate thermal conductivity, both Kersten-formulas should be used accordingly and not just one of them.

Due to the comparison between the calculated values according to Bertermann et al. (2014) and the measured TK04 thermal conductivity measurements, an approximation between the laboratory TK04 measurements and actual thermal soil properties could be made. The thermal conductivity values measured with the TK04 can be associated with a depth of 3–6 m based on the ThermoMap depth classification [7], which is in the depth range of very shallow geothermal systems like heat baskets. The collector systems are usually installed at a depth of 1.5 m, which corresponded to lower thermal conductivity values than those measured with the TK04 device. With the evaluated and soil-type-depending thermal conductivities, the system of shallow geothermal heat exchange can be understood more precisely. It should be noted that the measured thermal conductivity values for each grain size class in the mentioned depth represented conditions below the water surface as the TK04 measurements were performed under saturated conditions.

Author Contributions: Conceptualization, D.B.; Methodology, D.B., H.S., J.M., and S.F.; Software, J.M.; Validation, S.F. and J.M.; Formal Analysis, H.S.; Investigation, S.F.; Resources, D.B.; Writing—Original Draft Preparation, H.S. and S.F.; Writing—Review & Editing, D.B. and J.M.; Visualization, J.M.; Supervision, D.B.; Project Administration, D.B.; Funding Acquisition, D.B.

Funding: This work was co-funded by the European Commission: “ThermoMap” project (grant number 250446).

Acknowledgments: We want to thank our master’s students Christopher Weindl and Sebastian Claus for all their effort during the laboratory analysis and test field investigations. Further thanks to Viktor Iancu for cross-reading and discussions.

Conflicts of Interest: The authors declare no conflict of interest.

Nomenclature

λ [W (m·K) ⁻¹]	thermal conductivity (TC)
ϕ [-]	porosity
ρ_b [g cm ⁻³]	bulk density (BD)
ρ_s [g cm ⁻³]	density, soil components
θ_w [-]	water content (WC)
S_p [-]	amount of saturated pore volume
m_d [g]	mass, dry
θ [-]	degree of saturation
V_c [cm ³]	Volume, cylinder
n [cm ³]	volume, fraction of air
$\rho_{b, \text{eff}}$ [g cm ⁻³]	bulk density, effective
v_s [cm ³]	volume, fraction of solids
n_c [-]	amount of clay content

References

1. Bayer, P.; Saner, D.; Bolay, S.; Rybach, L.; Blum, P. Greenhouse gas emission savings of ground source heat pump systems in Europe: A review. *Renew. Sustain. Energy Rev.* **2012**, *16*, 1256–1267. [[CrossRef](#)]
2. Blum, P.; Campillo, G.; Münch, W.; Kölbl, T. CO₂ savings of ground source heat pump systems—A regional analysis. *Renew. Energy* **2010**, *35*, 122–127. [[CrossRef](#)]
3. Dickinson, J.; Jackson, T.; Matthews, M.; Cripps, A. The economic and environmental optimisation of integrating ground source energy systems into buildings. *Energy* **2009**, *34*, 2215–2222. [[CrossRef](#)]
4. Bense, V.F.; Kooi, H. Temporal and spatial variations of shallow subsurface temperature as a record of lateral variations in groundwater flow: Geothermal Data around Shallow Fault Zone. *J. Geophys. Res. Solid Earth* **2004**, *109*. [[CrossRef](#)]
5. Hähnlein, S.; Bayer, P.; Ferguson, G.; Blum, P. Sustainability and policy for the thermal use of shallow geothermal energy. *Energy Policy* **2013**, *59*, 914–925. [[CrossRef](#)]
6. Bertermann, D.; Bialas, C.; Morper-Busch, L.; Klug, H.; Rohn, J.; Stollhofen, M.P.; Jaudin, F.; Maragna, C.M.; Einarsson, G.M.; Vikingsson, S. ThermoMap—An open-source web mapping application for illustrating the very shallow geothermal potential in Europe and selected case study areas. In Proceedings of the European Geothermal Congress 2013, Pisa, Italy, 3–7 June 2013; pp. 1–7.
7. Bertermann, D.; Klug, H.; Morper-Busch, L.; Bialas, C. Modelling vSGPs (very shallow geothermal potentials) in selected CSAs (case study areas). *Energy* **2014**, *71*, 226–244. [[CrossRef](#)]
8. Bertermann, D.; Klug, H.; Morper-Busch, L. A pan-European planning basis for estimating the very shallow geothermal energy potentials. *Renew. Energy* **2015**, *75*, 335–347. [[CrossRef](#)]
9. Dehner, U. Bestimmung der thermischen Eigenschaften von Böden als Grundlage für die Erdwärmenutzung. *Mainz. Geowiss. Mitteilungen* **2007**, *35*, 159–186.
10. Hähnlein, S.; Bayer, P.; Blum, P. International legal status of the use of shallow geothermal energy. *Renew. Sustain. Energy Rev.* **2010**, *14*, 2611–2625. [[CrossRef](#)]
11. Salata, F.; Nardecchia, F.; Gugliermetti, F.; de Lieto Vollaro, A. How thermal conductivity of excavation materials affects the behavior of underground power cables. *Appl. Therm. Eng.* **2016**, *100*, 528–537. [[CrossRef](#)]

12. De Lieto Vollaro, R.; Fontana, L.; Vallati, A. Experimental study of thermal field deriving from an underground electrical power cable buried in non-homogeneous soils. *Appl. Therm. Eng.* **2014**, *62*, 390–397. [[CrossRef](#)]
13. De Lieto Vollaro, R.; Fontana, L.; Vallati, A. Thermal analysis of underground electrical power cables buried in non-homogeneous soils. *Appl. Therm. Eng.* **2011**, *31*, 772–778. [[CrossRef](#)]
14. Ocloń, P.; Cisek, P.; Rerak, M.; Taler, D.; Rao, R.V.; Vallati, A.; Pilarczyk, M. Thermal performance optimization of the underground power cable system by using a modified Jaya algorithm. *Int. J. Therm. Sci.* **2018**, *123*, 162–180. [[CrossRef](#)]
15. Janda, K.; Málek, J.; Recka, L. Influence of renewable energy sources on transmission networks in Central Europe. *Energy Policy* **2017**, *108*, 524–537. [[CrossRef](#)]
16. Komendantova, N.; Battaglini, A. Social Challenges of Electricity Transmission: Grid Deployment in Germany, the United Kingdom, and Belgium. *IEEE Power Energy Mag.* **2016**, *14*, 79–87. [[CrossRef](#)]
17. Gouda, O.E.S.; Osman, G.F.; Salem, W.; Arafa, S. Cyclic Loading of Underground Cables Including the Variations of Backfill Soil Thermal Resistivity and Specific Heat with Temperature Variation. *IEEE Trans. Power Deliv.* **2018**. [[CrossRef](#)]
18. Ocloń, P.; Bittelli, M.; Cisek, P.; Kroener, E.; Pilarczyk, M.; Taler, D.; Rao, R.V.; Vallati, A. The performance analysis of a new thermal backfill material for underground power cable system. *Appl. Therm. Eng.* **2016**, *108*, 233–250. [[CrossRef](#)]
19. Côté, J.; Konrad, J.-M. Thermal conductivity of base-course materials. *Can. Geotech. J.* **2005**, *42*, 61–78. [[CrossRef](#)]
20. Logsdon, S.D.; Green, T.R.; Bonta, J.V.; Seyfried, M.S.; Evett, S.R. Comparison of Electrical and Thermal Conductivities for Soils From Five States. *Soil Sci.* **2010**, *175*, 573–578. [[CrossRef](#)]
21. Ochsner, T.E.; Horton, R.; Ren, T. A new perspective on soil thermal properties. *Soil Sci. Soc. Am. J.* **2001**, *65*, 1641–1647. [[CrossRef](#)]
22. Clauser, C. *Einführung in Die Geophysik: Globale Physikalische Felder und Prozesse in der Erde*; Lehrbuch; Springer Spektrum: Berlin/Heidelberg, Germany, 2014; ISBN 978-3-642-04495-3.
23. Horai, K.; Simmons, G. Thermal conductivity of rock-forming minerals. *Earth Planet. Sci. Lett.* **1969**, *6*, 359–368. [[CrossRef](#)]
24. Kersten, M.S. Thermal Properties of Soils. Available online: <https://conservancy.umn.edu/handle/11299/124271> (accessed on 24 July 2018).
25. Chaudhari, P.R.; Ahire, D.V.; Ahire, V.D.; Chkravarty, M.; Maity, S. Soil bulk density as related to soil texture, organic matter content and available total nutrients of Coimbatore soil. *Int. J. Sci. Res. Publ.* **2013**, *3*, 1–8.
26. Saxton, K.E.; Rawls, W.J. Soil Water Characteristic Estimates by Texture and Organic Matter for Hydrologic Solutions. *Soil Sci. Soc. Am. J.* **2006**, *70*, 1569–1578. [[CrossRef](#)]
27. Abu-Hamdeh, N.H. Thermal Properties of Soils as affected by Density and Water Content. *Biosyst. Eng.* **2003**, *86*, 97–102. [[CrossRef](#)]
28. Abu-Hamdeh, N.H.; Reeder, R.C. Soil Thermal Conductivity Effects of Density, Moisture, Salt Concentration, and Organic Matter. *Soil Sci. Soc. Am. J.* **2000**, *64*, 1285–1290. [[CrossRef](#)]
29. Bertermann, D.; Schwarz, H. Laboratory device to analyse the impact of soil properties on electrical and thermal conductivity. *Int. Agrophys.* **2017**, *31*, 157–166. [[CrossRef](#)]
30. Farouki, O.T. *Thermal Properties of Soils*; Cold Regions Research and Engineering Laboratory: Hanover, NH, USA, 1981; p. 151.
31. Lu, S.; Ren, T.; Gong, Y.; Horton, R. An Improved Model for Predicting Soil Thermal Conductivity from Water Content at Room Temperature. *Soil Sci. Soc. Am. J.* **2007**, *71*, 8–14. [[CrossRef](#)]
32. Chen, S.X. Thermal conductivity of sands. *Heat Mass Transf.* **2008**, *44*, 1241–1246. [[CrossRef](#)]
33. Haigh, S.K. Thermal conductivity of sands. *Géotechnique* **2012**, *62*, 617–625. [[CrossRef](#)]
34. Lu, Y.; Lu, S.; Horton, R.; Ren, T. An Empirical Model for Estimating Soil Thermal Conductivity from Texture, Water Content, and Bulk Density. *Soil Sci. Soc. Am. J.* **2014**, *78*, 1859–1868. [[CrossRef](#)]
35. Markert, A.; Bohne, K.; Facklam, M.; Wessolek, G. Pedotransfer Functions of Soil Thermal Conductivity for the Textural Classes Sand, Silt, and Loam. *Soil Sci. Soc. Am. J.* **2017**, *81*, 1315–1327. [[CrossRef](#)]
36. Decagon Devices, Inc. *KD2 Pro Thermal Properties Analyzer—Operator’s Manual*; Decagon Devices, Inc.: Pullman, WA, USA, 2016; p. 71.

37. Seibertz, K.S.O.; Chirila, M.A.; Bumberger, J.; Dietrich, P.; Vienken, T. Development of in-aquifer heat testing for high resolution subsurface thermal-storage capability characterisation. *J. Hydrol.* **2016**, *534*, 113–123. [[CrossRef](#)]
38. United States Department of Agriculture. *USDA Textural Soil Classification*; Soil Mechanics Level 1; USDA: Washington, DC, USA, 1987.
39. Johansen, O. *Thermal Conductivity of Soils*; Corps of Engineers, U.S. Army, Cold Regions Research and Engineering Laboratory: Hanover, NH, USA, 1977.
40. Wessolek, G.; Stoffregen, H.; Täumer, K. Persistency of flow patterns in a water repellent sandy soil—Conclusions of TDR readings and a time-delayed double tracer experiment. *J. Hydrol.* **2009**, *375*, 524–535. [[CrossRef](#)]
41. Xiao, B.; Zhang, X.; Wang, W.; Long, G.; Chen, H.; Kang, H.; Ren, W. A Fractal Model for Water Flow through Unsaturated Porous Rocks. *Fractals* **2018**, *26*, 1840015. [[CrossRef](#)]
42. *Bodenkundliche Kartieranleitung: Mit 103 Tabellen und 31 Listen*, 5th ed.; Sponagel, H. (Ed.) Verbesserte und Erweiterte Auflage; E. Schweizerbart'sche Verlagsbuchhandlung (Nägele und Obermiller): Stuttgart, Germany, 2005; ISBN 978-3-510-95920-4.
43. Andersland, O.B.; Anderson, D.M. (Eds.) *Geotechnical Engineering for Cold Regions*; McGraw-Hill: New York, NY, USA, 1978; ISBN 0-07-001615-1.
44. Blackwell, J.H. A Transient-Flow Method for Determination of Thermal Constants of Insulating Materials in Bulk Part I—Theory. *J. Appl. Phys.* **1954**, *25*, 137–144. [[CrossRef](#)]
45. Davis, M.G.; Chapman, D.S.; Van Wagoner, T.M.; Armstrong, P.A. Thermal conductivity anisotropy of metasedimentary and igneous rocks. *J. Geophys. Res.* **2007**, *112*. [[CrossRef](#)]
46. Watson, D.F.; Philip, G.M. A refinement of inverse distance weighted interpolation. *Geo-Processing* **1985**, *2*, 315–327.
47. Park, J.; Santamarina, J.C. Revised Soil Classification System for Coarse-Fine Mixtures. *J. Geotech. Geoenviron. Eng.* **2017**, *143*, 04017039. [[CrossRef](#)]
48. Renger, M.; Bohne, K.; Facklam, M.; Harrach, T.; Riek, W.; Schäfer, W.; Wessolek, G.; Zacharias, S. *Ergebnisse und Vorschläge der DBG-Arbeitsgruppe „Kennwerte des Bodengefüges“ zur Schätzung bodenphysikalischer Kennwerte*; DBG-Arbeitsgruppe: Berlin, Germany, 2008.
49. Alrtimi, A.; Rouainia, M.; Haigh, S. Thermal conductivity of a sandy soil. *Appl. Therm. Eng.* **2016**, *106*, 551–560. [[CrossRef](#)]
50. Zhang, T.; Cai, G.; Liu, S.; Puppala, A.J. Investigation on thermal characteristics and prediction models of soils. *Int. J. Heat Mass Transf.* **2017**, *106*, 1074–1086. [[CrossRef](#)]
51. Cosenza, P.; Guérin, R.; Tabbagh, A. Relationship between thermal conductivity and water content of soils using numerical modelling. *Eur. J. Soil Sci.* **2003**, *54*, 581–588. [[CrossRef](#)]
52. Brigaud, F.; Vasseur, G. Mineralogy, porosity and fluid control on thermal conductivity of sedimentary rocks. *Geophys. J. Int.* **1989**, *98*, 525–542. [[CrossRef](#)]
53. Tarnawski, V.-R.; Leong, W.H. Thermal Conductivity of Soils at Very Low Moisture Content and Moderate Temperatures. *Transp. Porous Media* **2000**, *41*, 137–147. [[CrossRef](#)]
54. Ediger, V.Ş.; Hoşgör, E.; Sürmeli, A.N.; Tatlıdil, H. Fossil fuel sustainability index: An application of resource management. *Energy Policy* **2007**, *35*, 2969–2977. [[CrossRef](#)]
55. Fridleifsson, I.; Bertani, R.; Huenges, E.; Lund, J.W.; Rybach, L. *The Possible Role and Contribution of Geothermal Energy to the Mitigation of Climate Change*; Intergovernmental Panel on Climate Change (IPCC): Geneva, Switzerland, 2008; pp. 59–80.

